Frequency and Phase Mismatch Corrections for Imaging Interferometric Microscopy

P. Dey[1,2], A. Neumann[2], S. R. J. Brueck[1,2]

[1]University of New Mexico, Department of Electrical and Computer Engineering, Albuquerque, NM, USA
[2]University of New Mexico, Center for High Technology Materials, Albuquerque, NM, USA

ABSTRACT

Synthetic aperture Imaging Interferometric Microscopy (IIM) is a spatial resolution enhancement technique for optical microscopy. The technique involves combining multiple sub-images to achieve the resolution equivalent to that of a higher numerical aperture objective lens. Several image reconstruction challenges, including the frequency deviation in the sub-images and the lack of precision in maintaining mutual phase between sub-images, degrades the final output image quality. This paper proposes methods to correct the frequency deviation in sub-images and maintain the mutual phase between sub-images electronically. Structural Similarity Index Metric (SSIM) is used to compare the final simulation results. The methods are compared for a Manhattan structure of 260 nm spatial resolution with 2-µm pitch calibration grating on all sides. Both of these proposed methods are very useful in improving (by ~ 20%) the output image quality of IIM.

Keywords: Synthetic aperture interferometric microscopy, image reconstruction and enhancement.

1. INTRODUCTION

It has been demonstrated in previous work [1-2] that synthetic aperture optical imaging interferometric microscopy can successfully extend the resolution limit of optical microscopy to the linear systems limit of ~λ/4 using a low numerical aperture *(NA_{lens})* objective lens. This technique improves the resolution limit of the optical system by combining multiple off-axis illumination sub-images with a conventional on-axis coherent illumination microscopy image. The use of a low numerical aperture objective lens (NA_{lens}=0.4) ensures that the system retains a large depth of field, long working distance, and a wide field of view, [2] while enhancing the resolution. As is well known, the resolution limit of optical microscopy is proportional to the wavelength (λ) of the illumination source and inversely proportional to the numerical aperture (NA_{lens}) of the objective lens used in the system. As per Abbe, for the conventional on-axis coherent illumination microscopy, the highest spatial frequency passed through the optical system is λ/NA$_{lens}$ giving an effective resolution R ~0.5λ/NA_{lens} [3]. IIM technique extends the resolution limit of the system to R ~ 0.5λ/[NA_{lens} + sin(α_{ill})]. Here, α_{ill} is the off-axis illumination incidence angle. Illuminating the object at higher incidence angles allows the system to capture higher spatial frequency components that are important in increasing the resolution limit of the system. For a 0.4 NA_{lens} at λ= 532 nm (green laser source illumination), the limit of the system increases from ~650 nm (conventional microscopy limit) to ~200 nm (IIM limit) using α_{ill} =0°, 40°, and 80°. In this IIM case, the optical system achieves an effective numerical aperture of 1.38 ($NA_{effective}$ = 0.4 + 0.98) in the direction along the off-axis illumination. Next, the object is rotated 90° to reconstruct a 2D image of the targeted object. For Manhattan geometry objects, such as many IC patterns, there is less information in the diagonal directions, and this coverage is adequate, for more random features such as biological samples, additional sub-images need to be taken in the diagonal and perhaps other directions to fill in the frequency space information. For dark-field illumination conditions, sin(α_{ill}) > NA_{lens}, a reference beam at α_{ref} is introduced after the objective lens. For simulations we take a magnification (M) of unity; experimentally, α_{ref} = sin^{-1} (sin(α_{ill})/M).

Extending the resolution limit of optical microscopy will be helpful in the R2R micro and nanoscale device fabrication metrology. Optical microscopy is fast, non-contact, non-destructive, and can take real-time images over a large area. This unique feature makes the IIM techniques attractive for nanomanufacturing process control as an at-line metrology tool to scale appropriately for nanoscale devices with high precision and reliability. Using a higher power laser for imaging can reduce required integration time of the camera to get a high signal-to-noise ratio image. Hence, IIM system can be implemented as an in-line metrology tool in nanomanufacturing process by automating the IIM configuration changes.

2. CHALLENGES OF IIM

IIM extends the resolution limit of the optical system by combining multiple sub-images. However, major challenges of IIM include maintaining mutual frequency and phase between sub-images. Frequency deviation or shift in a sub-image occurs due to experimental errors in maintaining and matching the angles for the illumination (α_{ill}) and re-injected reference beam (α_{ref}). The frequency components are shifted in the reconstructed image and degrade the image quality. If we consider the off-axis illumination sub-image where the lens collects the higher diffracted orders (K= 2nd,3rd orders) and

reference beam (K=0th order) is re-injected in the image plane for interference as this is not going to be collected by the lens due to the incident illumination angle, then mathematically the intensity at the image plane can be described as [2]:

$$I = |E_0|^2 + |E_2|^2 + |E_3|^2 + 2|E_0E_2|\cos((2k_d + \triangle_f)x + k_0\varphi) + 2|E_0E_3|\cos((3k_d + \triangle_f)x + k_0\varphi) + 2|E_2E_3|\cos(k_dx) \quad (1)$$

Here, $\triangle_f = k_0$ [sin(α_{ill}) - sin(α_{ref})], denotes the sub-image frequency deviation due to angle mismatch between illumination and reference angles and φ is the overall phase mismatch. $k_0 = 2\pi/\lambda$ is the photon wave vector, $k_d = 2\pi/d$ is the grating wave vector with d the period of the Fourier component. The sub-images for IIM are combined in Fourier space and later returned to the spatial domain using an inverse Fourier transform. A frequency mismatch results in a compression/extension of the relevant part of the image; a phase mismatch misaligns the different frequency components of the image.

The sub-images are recorded separately and are independent of each other. These sub-images can have overall phase offsets. This extra phase appears in a sub-image because of the difference in the optical path length of the off-axis image and the reintroduced reference beam in the interference process. The path difference between the off-axis illumination path and reinjected reference beam path should be zero in an ideal case. In experiments, it is impossible to maintain equal path length to within a small fraction of an optical wavelength. As a result, maintaining a mutual phase between all the sub-images is challenging. This lack of precision in determining the mutual phase between sub-images impact the image quality of IIM. In the final IIM image reconstruction, each sub-image has an arbitrary phase shift which impacts the final image quality. The intent of the calibration grating is to provide the information for correcting these frequency and phase offsets.

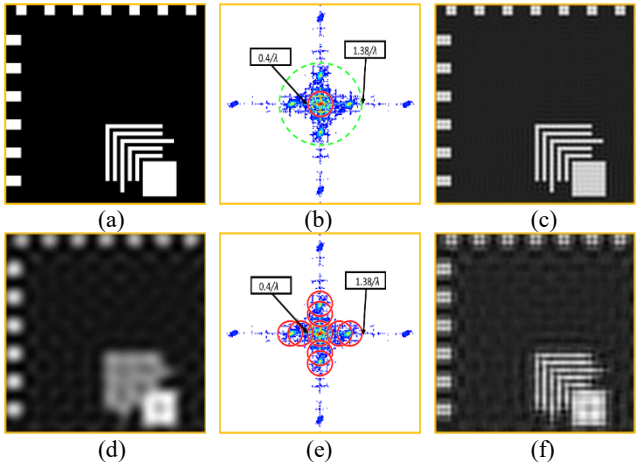

Fig. 1: (a) Manhattan structure with critical dimension, CD=260 nm, (b) Frequency space coverages for NA^* =1.38 objective lens (teal) and NA = 0.4 objective lens (red) with conventional on-axis coherent illumination microscopy, (c) Reconstructed image for conventional on-axis coherent illumination microscopy with NA^* =1.38 objective lens, (d) Reconstructed image for conventional on-axis coherent illumination microscopy with NA =0.4 objective lens, (e) Frequency space coverage for NA=0.4 and IIM system, and (f) Reconstructed image for IIM with NA=0.4 objective lens.

3. RESULTS OF FREQUENCY AND PHASE MISMATCH BETWEEN SUB-IMAGES

To illustrate the effects of frequency deviation and phase mismatch between sub-images in the IIM reconstructed image, we consider a Manhattan structure of critical dimension (CD) 260 nm as shown in Fig. 1(a). Sub-images (X_0: conventional on-axis microscopy image, X_1: α_{ill}=40° and $\theta_{sample\ rotation}$=0°, X_2: α_{ill}=80° and $\theta_{sample\ rotation}$=0°, Y_1: α_{ill}=40° and $\theta_{sample\ rotation}$=90°, and Y_2: α_{ill}=80° and $\theta_{sample\ rotation}$=90°) are created individually using NA =0.4 and λ =532 nm. Each sub-image (X_1, X_2, Y_1, and Y_2) frequency and phase are modified with random values in Fourier space. For frequency deviation consideration, the frequency components are shifted randomly between -5 pixels (~ -10°) to +5 pixels (~ 10°). The phase added to the sub-images is chosen randomly between -π to π radians. The on-axis conventional microscopy image (X_0) is considered perfect (free of frequency and phase deviations). The sub-images are then combined using the synthetic aperture approach. The reconstructed image is transformed back to the spatial domain. Some of the frequency components are present in multiple sub-images as a result of the frequency space overlap (Fig. 1(e)), so to have a uniform frequency response throughout the entire frequency space, linear rising and falling filters are used in the overlapping regions. The linear filters are chosen in such a way that the total filter response in the overlapping areas sums up to 1. This entire sub-image creation process is repeated several times with random frequency shifts and adding random extra phases in sub-images. The results of the variations after reconstruction

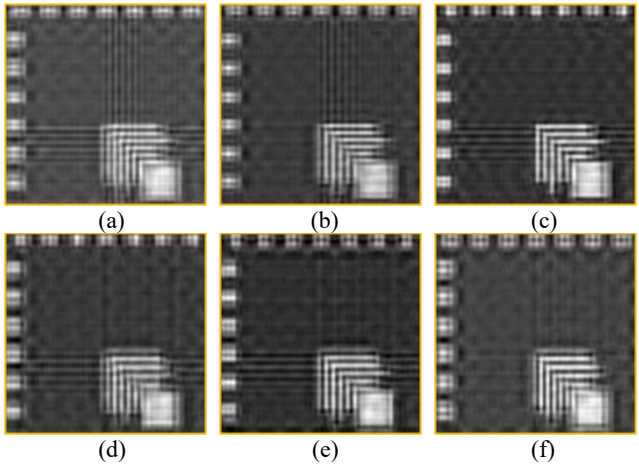

Fig.2:(FX_1,FX_2,FY_1,FY_2),(PX_1,PX_2,PY_1,PY_2) represent frequency deviations and arbitrarily added phases for X_1,X_2,Y_1 and Y_2 sub-images, respectively. (a):(0,4,2,1),(-3.141,-0.79,0.79,2.35); (b): (0,1,0,2),(3.14,0.79,0.79,0); (c):(2,0,0,0),(0,0,0,0.79); (d): (3,2,1,-4), (0.79,0,0,-0.79) ; (e) : (1,1,2,-2), (-0.79,0,2.35,-0.79); (f): (0,4,0,-4), (-2.35,3.14,-2.35,0)

are shown in Fig. 2. The reconstructed images have poor image quality compared to the ideal reconstructed image shown in Fig. 1(e). In some images, it is difficult to determine the actual number of nested 'ell' lines as the total number of lines are altered. These images are then compared with the reconstructed image of NA=1.38 (Fig. 1(c)). The SSIM values found after comparison are shown in Fig. 4(solid line). SSIM compares two images in terms of their intensity, contrast, and similarity.

4. PROPOSED METHODS FOR IMPROVING IMAGE QUALITY

To improve the image quality, we propose a method to correct frequency shifts in sub-images based on finding maximum cross-correlation between two consecutive sub-images in the overlapping regions. This correlation-based phase correction method is also used in holographic image formation [4]. In this work, we applied this correction procedure to improve the image quality of synthetic aperture imaging interferometric microscopy system. First, to correct the frequency deviation, the magnitude spectrum of consecutive sub-images is compared in the overlapping regions. The period of the side gratings in Fig.1 (a) is chosen so that all overlapping areas will have some common harmonics, which will help correct both frequency and phase shifts. The center frequencies of the sub-images are shifted from -5 pixels to +5 pixels with an increment of 1 pixel each time to estimate the location where the maximum correlation of the magnitude spectrums of the sub-images in the overlapping regions occurs. The second sub-image is then corrected accordingly based on the corresponding frequency shifts (m): $I_2(f)= I_2(f+m)$. Next, the median value of the phase difference ($k_0\varphi$) for two consecutive sub-images is calculated in the overlapping regions. The second sub-image frequency components are then multiplied with the additional phase to correct phase mismatch between sub-images: $I_2(f)= I_2(f)* e^{(-jk0\varphi)}$. This process is followed to correct all other sub-images.

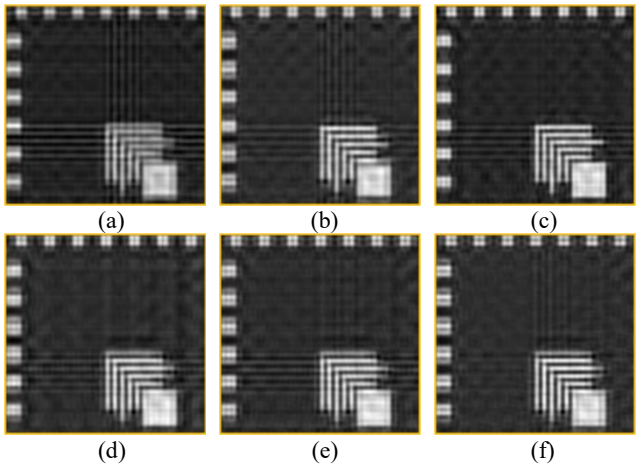

Fig.3: After applying correction methods- (a):(0,4,2,1),(-3.141,-0.79,0.79,2.35);(b):(0,1,0,2),(3.14,0.79,0.79,0);(c):(2,0,0,0),(0,0,0,0.79); (d):(3,2,1,-4),(0.79,0,0,-0.79); (e):(1,1,2,-2),(-0.79,0,2.35,-0.79); (f): (0,4,0,-4),(-2.35,3.14,-2.35,0)

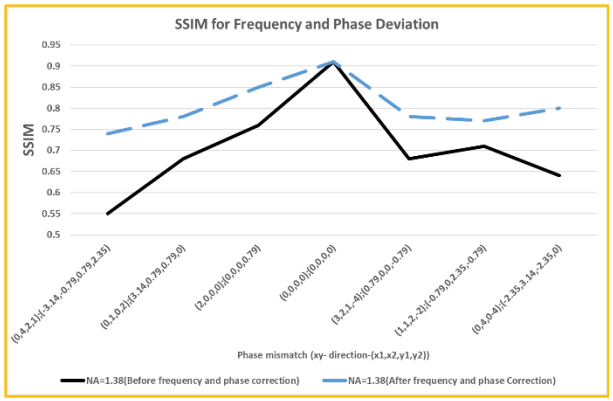

Fig.4: SSIM values for reconstructed images of Fig.2 (before applying correction methods – solid black line) and Fig.3 (after applying correction methods – dotted blue line).

The reconstructed images obtained after applying correction methods are shown in Fig. 3. Clearly, the quality of the images in Fig. 3 are better in comparison to the images of Fig.2. These images are compared with the 1.38 NA conventional microscopy image. SSIM values for reconstructed images after applying correction methods are shown in Fig. 4 (dotted line).

5. CONCLUSION

Frequency deviation and phase mismatch between sub-images reduces the IIM image quality. In some images, the total number of nested 'ell' lines are changed. From a visual inspection of the images, it is clear that the proposed correction methods significantly improve the image quality. In all scenarios, the images are cleaner, the nested 'ell' lines are easily detectable and are correct in number. The quantitative SSIM comparison confirms the image quality improvement. Correction methods can improve image quality by ~20%. The details of the effectiveness of this method in improving IIM experimental image quality will be discussed in a separate publication. Future research can be conducted to improve the image quality even more by increasing the dynamic range of the camera and correcting the aberration of the optical system.

REFERENCES

[1] A. Neumann, Y. Kuznetsova, S.R.J. Brueck, "Optical Resolution below λ/4 using synthetic aperture microscopy and evanescent-wave illumination," *Opt. Exp.*, 16, 20477-20483 (2008).

[2] A. Neumann, Y.Kuznetsova, S.R.J. Brueck, in *Optical Techniques for Solid-State Materials Characterization,* R.P.Prasankumar and A.J. Taylor, eds (CRC Press, 2011), pp. 533-574.

[3] M. Born and E. Wolf, *Principles of Optics* (Cambridge University Press, 2002).

[4] T. Gutzler, T.R. Hillman, S.A. Alexandrov, and D.D. Sampson, "Coherent aperture-synthesis, wide-field, high-resolution holographic microscopy of biological tissue," *Opt. Lett.*, 35, 1136-1138 (2010).